A COMPACT STORAGE RING FOR THE PRODUCTION OF EUV RADIATION

R.M. Bergmann, T. Bieri, P. Craievich, Y. Ekinci, T. Garvey, C. Gough, M. Negrazus, L. Rivkin, C. Rosenberg, L. Schulz, T. Schmidt, L. Stingelin, A. Streun, V. Vrankovic. A. Wrulich, A. Zandonella Callegher, R. Zennaro.

Paul Scherrer Institut,: 5232 Villigen, Switzerland.

We present the design of a compact synchrotron light source for the production of EUV radiation for metrology applications in the semiconductor industry. Stable, high brightness EUV light sources are of great potential interest for this industry. The recent availability of highly reflective mirrors at 13.5 nm wavelength makes EUV lithography a strong candidate for future generation semiconductor manufacture. Our design is based on a storage ring lattice employing design principles similar to those used in the new family of diffraction limited synchrotron radiation sources. The 430 MeV storage ring of circumference 25.8 m would have an emittance of ~ 6 nm-rad. The required EUV wavelength is obtained using a short period (16 mm) undulator.

I. INTRODUCTION

There is a consensus in the semiconductor manufacturing industry that extreme ultra-violet lithography (EUVL) is the most promising candidate for the next generation high volume manufacturing technique to produce smaller and faster integrated circuits. Recent advances in EUV plasma sources reaching 250 W EUV power at a wavelength of 13.5 nm (92 eV) and multi-layer molybdenum-silicon mirrors with high (70%) reflectivity and large (~ 2%) bandwidth at 13. 5 nm make this the wavelength of choice for EUVL. The development of metrology methods at EUV wavelengths for mask inspection will be indispensable for the eventual success of EUVL. The Paul Scherrer Institut (PSI) is currently developing an inspection tool for EUV photomasks on the XIL-II beamline of the Swiss Light Source [1]. However, the development of such an inspection tool is viable for commercialization only if a source of EUV radiation, having the required properties, such as high brightness, stability and compactness, and capable of being hosted in an industrial environment, can be developed. In this paper we describe a preliminary, novel design for a compact, low emittance synchrotron radiation source which will meet the needs of industry for mask inspection. Hereafter, the source will be referred to as COSAMI (Compact Storage ring for Actinic Mask Inspection).

II. SOURCE REQUIREMENTS

As the storage ring (SR) is operated for commercial purposes it is mandatory that it has a very high reliability. The Swiss Light Source (SLS) at PSI has a typical reliability figure of ~ 99% and we believe that this is sufficient for the semiconductor industry. However, as reliability is of such great importance our SR design will use only well-established accelerator technologies. In addition, as the SR will have a single user (i.e. it is not a research facility) and be installed in an industrial setting there is a strong emphasis on a 'compact' design, favoring reduced cost and foot-print. In general, compactness and low emittance are conflicting requirements and so to reach the required brightness we employ design techniques which are currently being used by the synchrotron radiation community to up-grade existing 3rd generation light sources to diffraction limited storage rings, i.e. the design is based on a multi-bend achromatic lattice [2]. In addition to the commercial constraints of size, cost and reliability the source must comply with the need to provide a mean power of ~ 10 mW on the mask with a substantial coherent fraction and with an intensity stability of 0.1% [3]. The power requirement converts to a source flux of 1.35×10^{15} photons/s/0.1% BW, assuming about 10% transmission from source to mask by an arrangement of mirrors. To provide a sufficient coherent fraction we aim for an emittance inferior to10 nm-rad. In order to meet the requirement of 10^{-3} stability we foresee to use the now familiar technique of "top-up" injection [4]. This implies the use of a full energy booster synchrotron.

To minimize the foot-print of COSAMI we have opted for a highly integrated system with the SR superimposed on the booster at a greater height. The linac injector is installed within the perimeter of the booster ring. A schematic of the facility is shown in Fig. 1.The size of the ring is mainly determined by, firstly, the beam

energy and the maximum tolerated magnetic field for the dipole magnets and, secondly, the straight section length for the undulator. The basic COSAMI parameters which will be discussed in the following sections are summarized in Table 1.

Table 1. Basic parameters of the compact EUV source

Parameter	Unit	value
Footprint	m^2	12×5
Circumference	m	25.8
Beam energy	MeV	430
Beam current	mA	150
Intensity stability	%	0.1
Radiation wavelength	nm	13.5
Flux	photons/s/0.1% BW	1.35×10^{15}
Brilliance	photons/s/mm^2/$mrad^2$/0.1% BW	1.8×10^{18}

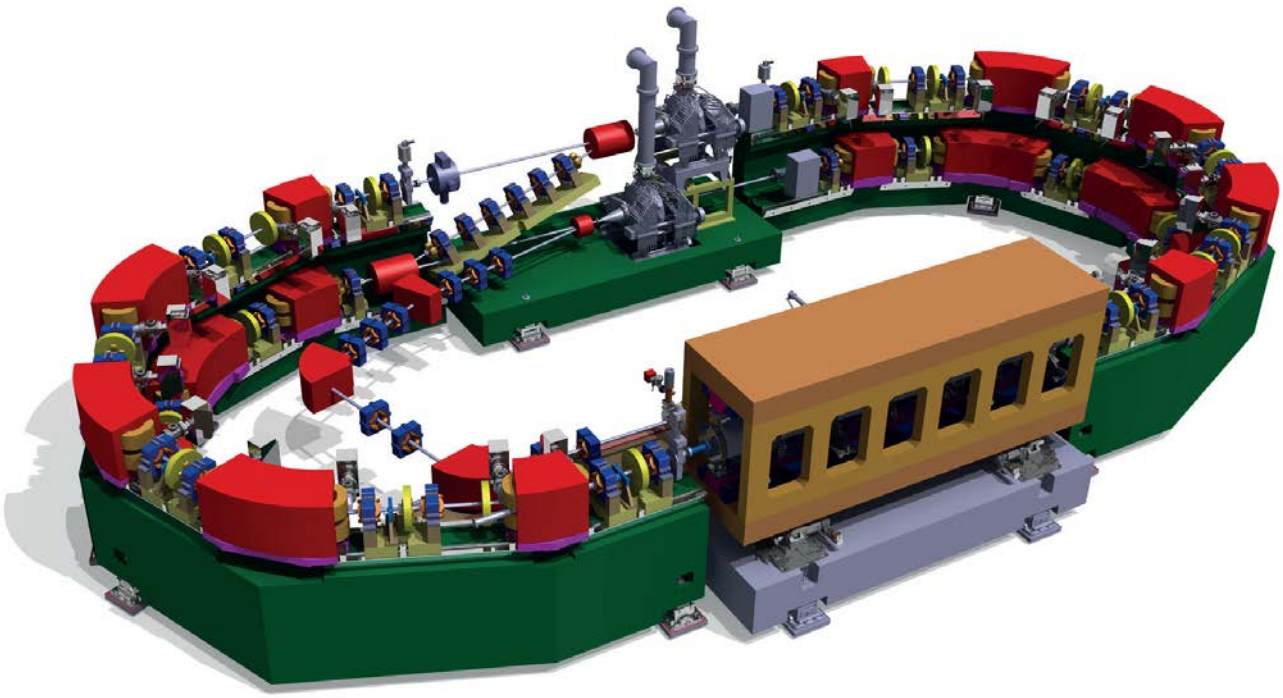

Figure 1:3-D schematic view of COSAMI. The storage ring is placed above the booster with the transfer line between them visible in the far straight section. The near straight section shows the frame which surrounds the undulator within it.

III. STORAGE RING DESIGN

Our source makes use of a single undulator installed in one four meter straight of a race-track configuration ring, the other straight being reserved for injection and installation of the RF cavity. The overall ring circumference is 25.8 m. Initial studies centered on the choice of undulator period, λ_u, and K parameter. This resulted in the choice of λ_u = 16 mm, and K = 0.63 (peak on-axis magnetic field of 0.42 T). With these fixed, the storage ring energy (430 MeV) is defined to provide the desired wavelength and the minimum current (95 mA) and undulator length (~ 3.2 m) to provide the required flux. To have some margin we choose a design current of 150 mA which we believe is suitably low to avoid detrimental collective effects. Further details can be found in Ref. 5.

Although designs for both the booster and SR optics, and for the transfer line between them, exist we will concentrate here on the design of the SR. Details of the booster and transfer line can be found in Ref. 6. The storage ring has a low-emittance lattice with rather strong horizontal focusing. The compactness of the facility results in a dense lattice of the multi-bend achromat type

with strong quadrupoles of short focal length and strong sextupoles to compensate the chromaticity introduced by the quadrupoles. High magnet gradients require small magnet apertures, and therefore small beam pipe dimensions: an elliptic cross section of 30 × 20 mm^2 full width × height was chosen. Thanks to the low peak dispersion in a multi-bend achromat lattice a large momentum acceptance is provided even at reduced beam pipe aperture, thus reducing the loss of particles that experience Touschek scattering. Due to the high particle density in a low emittance ring Touschek scattering dominates the beam lifetime. Therefore, the vertical emittance, which is small by nature in a synchrotron, is increased deliberately to a few percent of the horizontal emittance in order to reduce the bunch particle density. Scattering from residual gas atoms also contributes to the beam lifetime. The two arcs are 5-bend achromats with rather strong horizontal and low vertical focusing as is typical for low emittance lattices. Twelve identical blocks are used, one between each adjacent bending magnets and one at both ends of the straight sections. Each block is composed of a pair of quadrupoles either side of a sextupole, a combined horizontal/vertical corrector and a beam position monitor (BPM). This arrangement provides maximum dispersion and good betatron de-coupling for chromaticity correction, and orthogonal correctors for orbit correction. Gradients in the bending magnets provide the vertical focusing in order to (a) save space and (b) increase the horizontal damping to further reduce the emittance. Skew quadrupole windings in the sextupoles generate closed bumps of vertical dispersion in order to create a convenient amount of vertical emittance. Figure 2 shows the optical functions: the horizontal beta-function is almost periodic in the arcs with small values in the bending magnets to generate a low emittance, small in the undulator to get high coherence by optimum matching to the diffraction phase-space, and large in the injection straight to allow for a maximum offset of the injected beam. To reduce particle losses due to Coulomb scattering, the vertical beta function is minimized at the undulator edges, taking into account the undulator's vertical focusing, which is not negligible at this low energy. The working point is shown in the tune diagram of figure 3 taking into account constraints from injection and dynamic aperture optimization. It may be smoothly varied within ±0.15 in both planes while keeping the maximum beta functions below 20 m, straight section dispersion below 5 cm and emittance below 8 nm. The essential parameters of the storage ring are summarized in Table 2.

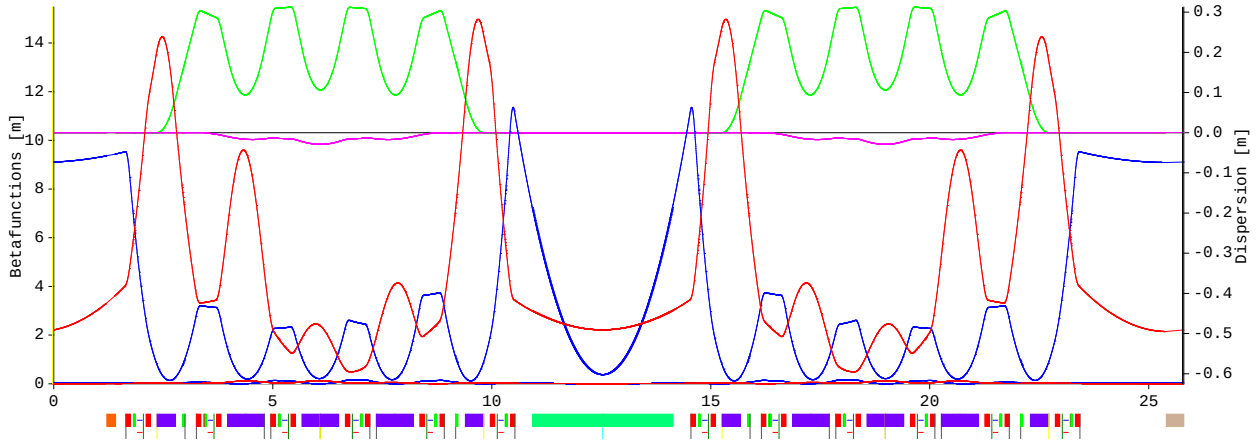

Figure 2: Storage ring optical functions (β_x , β_y , D_x, D_y). Bending magnet positions are indicated in blue. The undulator is represented by the green bar.

For ease of alignment and improved stability the storage ring elements would be combined on girders. We assume ten girders each supporting one magnet and one quadrupole-sextupole-corrector-BPM block. For readily achievable misalignment errors; 100 µm in absolute girder position, 50 µm offset girder-to-girder, 50 µm element-to-girder misalignment and 100 µrad roll errors simulations show that orbit correction can be achieved with corrector strengths of no more than 1 mrad in both planes.

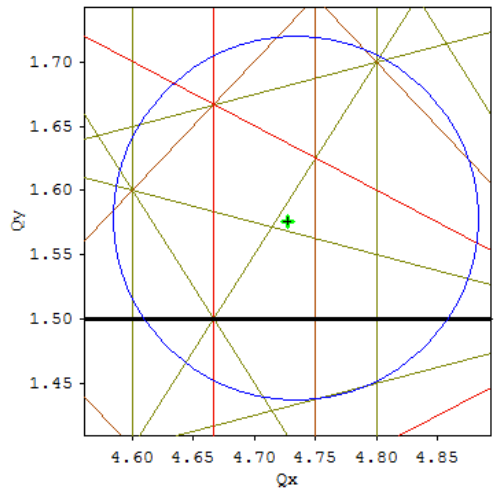

Figure 3**:** Tune diagram showing regular resonances up to 5th order: working point (✚) and range of tune variation (○).

Table 2 Storage ring parameters

Circumference	25.8 m
Energy	430 MeV
Working point $Q_{x/y}$	4.73 / 1.58
Energy loss/turn	2.83 keV
Emittance	5.5 nm-rad
Natural chromaticities $\xi_{x/y}$	-9.7 / -6.9
Momentum compaction α_c	0.0258
Relative energy spread	4.13 x 10-^{4}
Hor. damping partition J_x	1.54
Damping times $\tau_{x/y/E}$ (ms)	16.6. / 25.6 /17.5

IV. BEAM LIFE-TIME

IV.A. Touschek scattering

The loss rate due to Touschek scattering is proportional to the particle density in the bunch, and it is a steep inverse function of the momentum acceptance, which allows scattered particles to be captured. Momentum acceptance is given by the RF voltage and by the off-momentum lattice acceptance. The lattice acceptance is the (momentum dependent) dynamic acceptance obtained, including aperture limitations from the beam pipe. Touschek lifetime as a function of RF voltage exhibits a maximum when the RF momentum acceptance meets the lattice momentum acceptance. For higher RF voltages a shorter bunch length will lead to lower lifetime.

As discussed above, to deliver the required EUV power, 150 mA of current will be nominally stored in COSAMI. For a RF cavity frequency of 500 MHz the 25.8 m circumference corresponds to 43 “buckets”, however a rather large gap is required for clearing trapped ions and the full current is distributed over 24 bunches only. The vertical emittance, small by nature, will be excited by means of a vertical dispersion bump to about 10% of the horizontal emittance in order to reduce the bunch density.

Positive ions, created by beam-gas scattering, can be trapped by the Coulomb potential of the electron beam. This can result in several detrimental effects such as emittance increase, tune shifts and tune spread which can, in turn, excite non-linear resonances. This effect can be mitigated by introducing a gap in the electron bunch fill pattern. Hence the reason why we consider distributing the current over 24 bunches thus leaving a gap of 40 ns in the time structure. Alternatively, if this proves insufficient, “clearing” electrodes can be installed in the ring to sweep the positive ions out of the vacuum chamber. A detailed study of ion-trapping in COSAMI is given in Ref. 7.

An RF voltage of 400 kV gives 2.3% of momentum acceptance which is slightly larger than the minimum values of the lattice momentum acceptance. The calculation of beam lif-time includes a 12 mm aperture restriction from the injection septum and the 7 mm gap from the undulator, which affects the Coulomb scattering losses. At an emittance coupling of 10% the Touschek lifetime thus obtained is 17 minutes. The lifetime from residual gas scattering, assuming carbon monoxide at $2{\cdot}10^{-9}$ mbar partial pressure, is 2.2 hrs for Coulomb scattering and 37 hrs for bremsstrahlung. This gives a total lifetime of 15 minutes.

IV.B. Intra- beam scattering (IBS)

IBS leads to a blow up of the bunch in all six dimensions. For the case of 8.3 mA per bunch (i.e. 200 mA in 24 bunches) and 10% coupling, the horizontal emittance would increase by approximately one third, and the energy spread by one half. The vertical emittance would follow the horizontal one for a given coupling, but the coupling can be regulated. The resulting doubling of the bunch volume doubles the Touschek lifetime too, thus giving a total lifetime of 26 minutes.

A 3rd harmonic cavity would stretch the bunches by a factor of ≈2.5 (beam loading would result in some variation along the bunch train) and lower the bunch density correspondingly, thus reducing both Touschek scattering and IBS-blow-up. In this case the lifetime would become approximately 30 minutes at a reduced emittance increase of only 20%. Finally, after some period of vacuum chamber surface cleaning, a reduction of the ion clearing gap to 11 RF buckets might be feasible at the nominal current of 150 mA and a total lifetime of about one hour may be expected.

VI. MAGNETS

The SR lattice has been optimized to minimise the number of magnet types. In view of the need to produce a compact design there is a strong incentive to economise on space by combing more than one function in some magnets. For example, the sextupole magnet has an additional skew-quadrupole winding. The storage ring magnets are made from solid iron, whereas in the booster laminated magnets are used in order to reduce the effects of eddy currents. The SR bending magnets have only one type of gradient profile with an integrated sextupole component. Based on this profile four units of 420 mm length provide the four end bends (22.5°) and six units of 840 mm length provide the main bends (45°). The bending magnets are of the sector type. Conceptual designs exist for the dipole, quadrupole, sextupole and corrector magnets needed for both the SR and booster ring. For illustration, Fig. 4 shows a schematic of the quadrupole design. The storage ring magnet parameters are summarized in Table 3.

.

Table 3. Storage ring magnet parameters

Type	# pieces	L (mm)	B (T)	B' (T/m)	1/2B'' (T/m^2)
Gradient bend, solid iron	4/6	420/840	1.34	-4.10	-17.1
quadrupole	24	100	0	30	0
Sextupole	16	50	0	$\pm 3.0^{skew}$	580
H/V corrector magnet	12	80	± 0.018	0	0

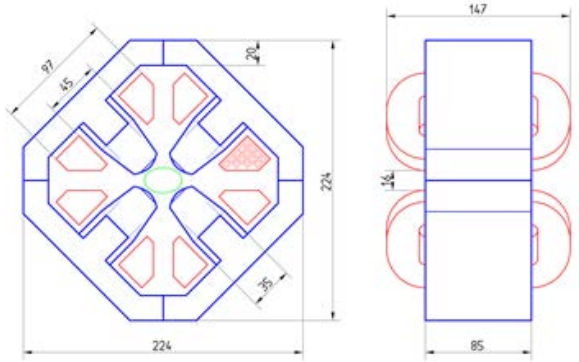

Figure 4. Schematic of quadrupole design. Dimensions are in mm.

V. THE UNDULATOR

The undulator will operate on the fundamental resonance in order to provide the 13.5 nm radiation. Assuming the IBS increased emittance, the convolution of the electron beam and diffraction phase spaces give a photon beam emittance of 8.1 nm horizontal and 2.3 nm vertical. The source point properties are 55 × 50 μm^2 rms size and 145 × 50 μrad^2 rms divergence. The proposed undulator for COSAMI is based on previous undulator construction experience at PSI for the SLS and SwissFEL. Even though the maximum field, 0.42 T, is moderate, the short period length of 16 mm combined with a minimum vacuum stay clear aperture of 7 mm requires strong magnets and a minimized space for the vacuum chamber. The undulator will be a fixed energy, fixed gap, in-vacuum undulator with a hybrid magnet structure. The magnetic design is adapted from the SwissFEL U15 in-vacuum undulator. In contrary to the single pass FEL, for COSAMI a good field integral region of ± 12mm is required, which is included in the magnet design. The pole tip width of the U16 has to be increased from 15mm to 30mm and hence also the magnet width has to be enlarged from 30mm to 40mm. The magnetic material will be the same as for U15: NdFeB magnets optimized with diffused Dy which provide, at room temperature, the best combination of magnet strength, B_r and stability which is closely linked to the coercitivity. A high coercitivity prevents the magnets from de-magnetizing due to electron-loss induced radiation. The poles are from a cobalt iron alloy with a saturation magnetization of 2.35T. Calculation shows that the required field can be realized with a gap of about 8mm. For the highest photon flux, the entire central cone of the fundamental of the emitted light has to be focused to the sample. The flux is $1.4 \cdot 10^{15}$ photons/sec/0.1% bandwidth.
The U16 as briefly outlined here is a state of the art undulator which guarantees the required performance for reliable operation of COSAMI.

VII. THE VACUUM SYSTEM

To achieve sufficient beam lifetime the average vacuum pressure has to be in the 10^{-9} mbar range (CO equivalent). The design goal for the COSAMI vacuum system is to achieve this value after commissioning with an integrated beam dose of 100 Ampere-hours. For the calculation of the vacuum pressure profile the program Molflow+ [8] was used. A 3D-model with dimensions of one full arc (30 mm × 20 mm transverse, 8.8 m long) was used as input for the simulation The calculation of the photo desorption was done with the program Synrad+. Both programs, Molflow+ and Synrad+, use the same 3D-model as input. The accumulated photon dose which is calculated in Synrad+ can be imported into Molflow+ to

calculate the desorption rate for each vacuum chamber element.

The vacuum chamber model is equipped with a total of ten pumping ports for the connection of lumped pumps. On each pumping port a pump providing a total pumping speed of 20 l/s is attached. The pressure profile was calculated with Molflow+for several beam dose rates.

Many simulations have been done to arrive at a satisfactory solution which fulfills the design requirements. The best solution for a vacuum pipe with elliptical cross section of $30 \times 20 mm^2$ was achieved with 10 sputter ion pumps and a full NEG coating of the inner tube surface. In this configuration an average pressure of 10^{-9} mbar CO equivalent can be achieved with an accumulated beam dose of 100 Ah.

The simulation is a conservative approach because in the Molflow+ calculations the pumping speed of the NEG coated surfaces were not taken into account. Only the improvement of the reduced photo desorption yield was included. This gives a safety margin and allows one to achieve the design goals even with full saturation of the NEG surface.

VII.A. Chamber design

Due to the relatively low beam energy the COSAMI vacuum chambers have a low longitudinal heat load distribution and a simple cooling channel design. Thus stainless steel is the most appropriate choice of chamber material. Five vacuum chambers, with a total length of 8.8 m, form one arc of the COSAMI lattice, Fig. 5. The standard vacuum tube has an elliptical cross section of 30 mm × 20 mm, a wall thickness of 1 mm, and is made from 316L stainless steel. The connections are done with CF flanges made from 316 LN stainless steel.

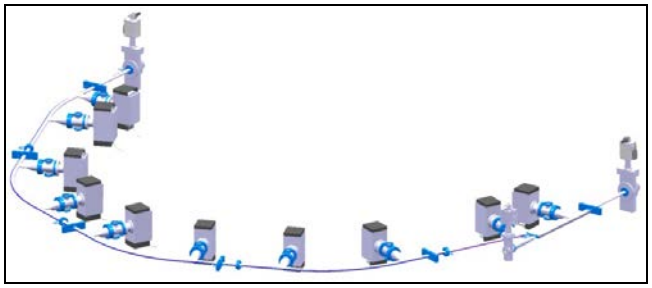

Figure 5. Vacuum chamber layout for one arc.

Ten lumped pumps are attached to the vacuum chambers of one arc on the inside of the storage ring. All pressure calculations have been done with a pumping speed of 20 l/s per pump. The pump ports on the vacuum chamber have an inner tube diameter of 65 mm which make it possible to install sputter ion pumps of the diode type with 55 l/s nominal pumping speed. If more detailed considerations lead to the conclusion that a higher pumping speed is required then these pumps can be replaced with sputter ion / NEG pump combinations with a pumping speed of 200 l/s.

VIII. LINAC INJECTOR

Radio-frequency injector linacs for storage rings normally employ travelling wave RF structures for acceleration. These have to be preceded by high voltage (~ 100 kV) thermionic guns, as electron source, followed by bunching cavities at a sub-harmonic and the fundamental frequency of the main accelerating structure. Such injectors, once equipped with the necessary diagnostics tend to be rather long (~ 12 m) [9]. For COSAMI, we propose to use a photo-injector to provide beam for the booster. Photo-injectors are, by now, a well-established technology and are employed in several user facilities, notably short-wavelength free electron lasers with highly reliable performance. The use of cesium-telluride photo-cathodes, with their high quantum efficiency, mean that modest power lasers, readily available commercially, can provide the laser energy required for the electron beam.
We propose to use a C-band (5.7 GHz) travelling wave structure, based on the technology developed for the RF linac of SwissFEL. The structure would be made of 113 cells with a $2\pi/3$ phase advance per cell. The overall length would be ~ 2.1 m. The first three cells have to be adjusted in length with respect to the others to ensure synchronism with the RF wave at low beam energy, Fig 6. Simulations show that the structure, driven by a 20 MW peak-power klystron, can easily produce a beam of 43 MeV having the required characteristics of emittance, energy spread and bunch length needed for injection into the booster ring. Further details can be found in Ref. 10.

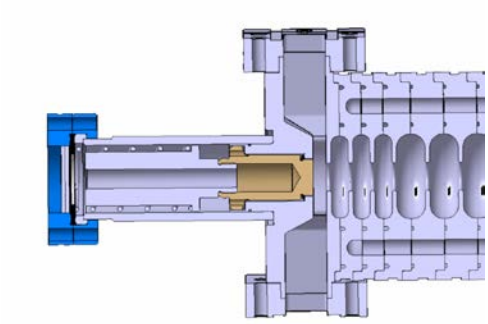

Figure 6. Schematic of the first six cells of the C-band travelling wave gun.

IX. RF SYSTEM

Detailed studies of the radio-frequency hardware for COSAMI have been carried out. Commercially available equipment appears to meet the needs of both the booster and SR RF systems. Each ring would use a single 500 MHz standing-wave cavity of the type developed for the ELETTRA storage ring [11]. A large cavity voltage (400 kV) is required to ensure adequate momentum acceptance and beam life-time, resulting in cavity wall losses of 24 kW. A single solid state amplifier delivering 35 kW continuous power would be sufficient to drive both the booster and SR cavities via 6-1/8" EIA co-axial transmission lines. As the radiated synchrotron power is low (~ 420 W) the cavity coupling is close to1.0. A summary of relevant parameters for the SR RF system is shown in Table 4.

Table 4: Storage ring RF parameters

Revolution frequency	11.62 MHz
RF frequency	499.8 MHz
Harmonic number	43
Cavity Q factor	40,000
Shunt impedance	3.4 MΩ
Cavity wall losses	24 kW
Gap voltage	400 kV
Energy loss/turn	2.83 keV
Overvoltage	141
Synchronous phase	0.4°
Synchrotron frequency	148 kHz
Bunch length	11 ps
Radiated power (@ 150 mA)	420 W
Coupling factor	~ 1.02

Simulations have been performed to evaluate the effects of longitudinal single bunch instabilities and longitudinal and transverse coupled-bunch instabilities. Resistive wall effects can excite the so-called microwave instability limiting the single bunch current. Simulations with the code MBTRACK [12] indicate that the COSAMI single bunch current is below the threshold of the microwave instability. As noted in section IV.B the use of a 3rd harmonic cavity would increase the Touschek life-time via the increase in bunch length and concomitant reduction in bunch density. The reduction in peak single-bunch current would also increase considerably the threshold for the microwave instability. The higher order modes (HOM) of the RF cavity can drive longitudinal and/or transverse instabilities when the HOM frequencies match, respectively, synchrotron or betatron sidebands in the beam spectrum. The HOM spectrum of the 500 MHz cavity is well known from measurements on ELETTRA and SLS. One can mitigate HOM effects to some extent by adjusting the HOM frequencies by varying the cavity temperature. However, to ensure that coupled bunch instabilities do not limit the beam intensity it would appear that a multi-bunch feedback system may be needed for COSAMI. Further details are available in Ref. 6.

X. SHIELDING

The operation of a EUV source in an industrial setting would require sufficient shielding to protect personnel from the harmful effects of ionizing radiations generated by the source. We present here a very preliminary, non optimized, study of the shielding requirements of COSAMI in order to reduce radiation levels below regulatory limits. Two approaches have been studied; one in which extensive use of local shielding is used around areas where particle losses are more likely and a second using global "wall" shielding around the facility. As one might expect, the local shielding approach allows one to reduce the mass of shielding material. However, locally shielding certain areas of the SR makes access for maintenance more complex and, for this reason, we treat only the wall shielding approach in this paper. A comparison of both approaches is available in Ref. 6. Shielding calculations have been performed using the Monte Carlo particle transport code MCNP 6.1 [13]. The model is illustrated in Fig. 7 and includes the SR, magnets, vacuum chamber, undulator and collimator. The beam life-time, current and energy are used to calculate an electron loss rate (1.2 × 108 electrons/s) This loss rate is then converted to dose rates in MCNP using conversion data from the International Commission on Radiological Protection agency.

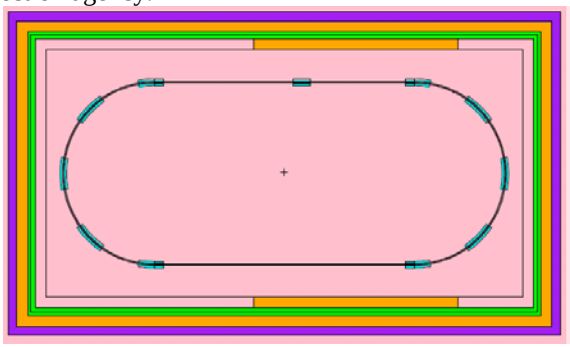

Figure **7** : A horizontal slice of the MCNP model for the wall shielding concept. Materials: Concrete (purple), lead (green), borated polyethylene (orange), air (pink), and magnet material {equal parts Cu and Fe} (light blue).

The main contributor to high energy photon production is bremsstrahlung, which can go on to create neutrons from photonuclear interactions in the magnet and shielding materials. The photons are forward-peaked and exist mainly in the horizontal ring plane. To shield these photons, thicknesses of lead were chosen to produce the most compact design. Lead has some photonuclear yield, however, and therefore the neutron shielding should always be placed behind the lead shields. The neutron

shielding material was chosen to be high density polyethylene since it has the highest hydrogen density of any common material. Hydrogen produces 2.2 MeV photons when it absorbs a neutron, however, so it is recommended that borated polyethylene (at least 5wt% boron) be used as a shielding material. This allows the hydrogen to moderate the neutrons, but the boron is the dominant absorber and therefore suppresses secondary photon emission via its large (n,α) cross section.

The wall shielding version assumes that losses are split between four loss points: 40% at the collimator just after the injection point, 10% at the upstream undulator face, 50% distributed evenly around the ring, and an extra 20% at the injection point to account for injection errors. The neutron shielding is 30 wt% borated polyethylene and the photon shielding is lead. The walls and ceiling are both covered in a constant thickness of both materials (lead before the plastic), and the height of the first shielding layer is kept constant at 3 m from the floor for every thickness considered. Lead 'plugs' downstream of loss points are used, including one downstream of the injection loss point that extends onto the ceiling due to the vertical component in the injection angle. An additional thickness of polyethylene is also used near the collimator and undulator loss points. The thin lead layer is 7 cm thick and the lead plugs are 15 cm thick. The general polyethylene layer is 25cm thick, but around the undulator and the collimator it is 60 cm thick. Figure 8 shows the dose rate maps for the wall shielding concept. The increase in beam life-time that a 3rd harmonic cavity would bring would result in a reduction in the particle loss rate thus permitting some relaxation in the shielding layout.

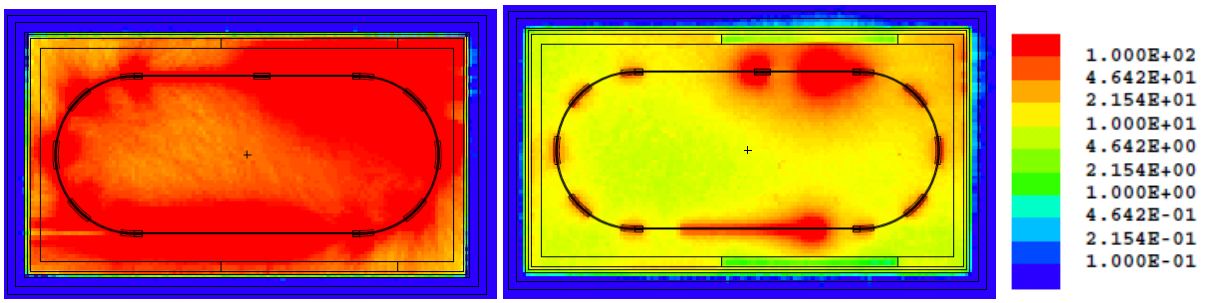

Figure 8**.** Dose rate maps for [left] photons and [right] neutrons using the wall shielding concept. The plane corresponds to a height of 2.15 m, where the collimator is. The units are in μSv/hr with blue regions showing all areas below 0.1 and red regions showing all areas above 200 μSV/hr.

XI. CONCLUSIONS AND OUTLOOK

We have presented a preliminary design of a comapact EUV radiation source which may be of interest to the semiconductor industry. The design appears to meet the brightness, stability and compactness requirements expected of such a source. Although we have not discussed all possible sub-systems of such a facility, e.g. diagnostics, control systems, power supplies, we believe that the systems not treated have readily available solutions from industry. The one exception is injection into the storage ring. There is limited space available in the injection straight for the kicker magnets of a conventional 4-bump injection scheme. In addition, the short revolution time of the compact ring requires very fast kickers, which present a considerable challenge. In the absence of a clear solution we have preferred not to cover this topic here. Future studies will address this problem.

ACKNOWLEDGMENTS

This work has been partially financed by a grant from the Swiss Commission for Technology and Innovation (Grant # 19193.1PFNM-NM). Thanks are due to Masamitsu Aiba for discussions on injection problems and to Michael Ehrlichman for IBS calculations and for bringing our attention to the ion-trapping possibility.. We thank the company Advanced Accelerator Technologies AG for their participation in the production of 3-D CAD drawings.

REFERENCES

1. R. RAJEEV et. al., "Towards a stand-alone high-throughput EUV actinic photomask inspection tool – RESCAN" Metrology, Inspection and Process Control for Microlithography XXXI, Ed. M.I. Sanchez and V.A. Ukraintsev. Proc of SPIE Vol 10145, 2017.
2. P.F. TAVARES, S.C. LEEMANN, M. SJÖSTRÖM and Å. ANDERSSON, "The MAX IV storage ring project", Journal of Synchrotron Radiation, Vol 21, pp 862-877, 2014.
3. I. MOHACSI, P. HELFENSTEIN, R. RAJENDRAN and Y. EKINCI, "Scanning Scattering Contrast Microscopy for Actinic Mask Inspection," Metrology, Inspection and Process Control for

Microlithography XXX, Ed. M.I. Sanchez and V.A. Ukraintsev. Proc. of SPIE Vol 9778, 2016.
4. A. LUDEKE et. al., “Status of the Swiss Light Source”, Proceedings of the 10th European Particle Accelerator Conference (Edinburgh), pp3424-3426, 2006.
5. A. WRULICH, Y. EKINCI, S. LEE and L. RIVKIN, “A Feasibility Study for COSAMI – a Compact EUV Source for Actinic Mask Inspection” *PSI Internal Report, un-published.*
6. M. AIBA et. al., “COSAMI Feasibility Study” *PSI Internal Report*, January 2017.
7. A. WRULICH, “Ion trapping”, PSI Technical Note, unpublished.
8. M. ADY, R. KERSEVAN and M. GRABSKI “Monte Carlo simulations of synchrotron radiation and vacuum performance of the MAX IV light source”, Proceedings of the 5th International Particle Accelerator Conference (Dresden), pp2344-47, 2014.
9. M. PEDROZZI et. al., “Commissioning of the SLS Linac”, Proceedings of the 7th European Particle Accelerator Conference (Vienna), pp 851-853, 2000.
10. R. ZENNARO, P. CRAIEVICH, C. HAURI, L. STINGELIN, A TRISORIO and C VICARIO, “Compact Electron RF Travelling Wave Gun Photo Injector” Proceedings of the 8th International Particle Accelerator Conference (Copenhagen), pp 1550-52, 2017.
11. A. MASSAROTTI et. al., ‘500 MHz cavities for the Trieste synchrotron light source ELETTRA”, Proceedings of the 2nd European Particle Accelerator Conference (Nice), pp 919-921, 1990.
12. G. SKRIPKA et. al., “Simultaneous Computation of Intrabunch and Interbunch Collective Beam Motions in Storage Rings”, Nuclear Instruments and Methods A, Vol 806, pp 221-230, 2016.
13. D.B. PELOWITZ, “MCNPX manual, version 2.7.0”, Los Alamos report LA-CP-11-00438, April 2011.